Observation of Reduced Heat Transport inside the Magnetic Island O Point in the Large Helical Device

S. Inagaki, N. Tamura, K. Ida, Y. Nagayama, K. Kawahata, S. Sudo, T. Morisaki, K. Tanaka, T. Tokuzawa, and the LHD Experimental Group

National Institute for Fusion Science, 322-6 Orhoshi-Cho, Toki-City, 509-5292 Japan

(Received 6 December 2002; published 5 February 2004)

Evidence for a reduction of heat transport inside the magnetic island O point is observed from the propagation of a cold pulse produced by a tracer encapsulated solid pellet in the Large Helical Device. A small peak and slow propagation of the cold pulse are observed inside the island. A significant result is that electron heat diffusivity inside the island is estimated to be 0.2 m^2/s which is smaller than that outside the island by an order of magnitude.

DOI: 10.1103/PhysRevLett.92.055002 PACS numbers: 52.55.Dy, 52.25.Fi

It is believed that magnetic islands may deteriorate plasma confinement considerably because of the flattening of profiles [1,2]. In general, flattening of electron and ion temperature profiles inside magnetic island O points is observed in the Large Helical Device (LHD) as well as tokamaks [3–6]. Profile flattening, however, does not indicate a deterioration of the cross-field heat transport inside the magnetic island. The heat flows radially along a boundary of magnetic island by parallel heat transport. Therefore the temperature profiles are expected to flatten over an island unless there are significant heat sources or sinks inside the island [7,8]. Since transport barriers at or near the rational surfaces have been observed in tokamak plasmas [9,10], the transport of the magnetic island itself has come to be considered important as well as the dynamics of the island [11]. The roles of the magnetic island on particle and momentum transport are investigated both in tokamaks and in helical systems. In fact, density profile peaking inside the magnetic island has been observed in Joint European Torus [4]. Moreover shear flow inside the magnetic island is clearly observed in the LHD [3]. These observations suggest that particle and momentum transport are small inside the magnetic island, and they imply that the cross-field heat transport is also small inside the island. In spite of the importance of heat transport, a direct experimental result of cross-field heat transport inside the island has not been reported. This is because the temperature gradient is almost zero inside the magnetic island and therefore static transport analysis based on the temperature gradient and radial heat flux is invalid for estimating the heat diffusivity across the magnetic island. Hence a transient transport experiment is required to estimate the heat diffusivity inside the island. In general, a spontaneous island rotates in the laboratory frame due to the $E \times B$ drift. This rotation makes analysis of the transient response difficult. The nonrotating island produced by external perturbation coil currents is considered to be ideal for the transient transport analysis because the interaction between the dynamics inside the island and the motion of the island itself can be eliminated. This Letter presents the first result of perturbative transport analysis for the heat transport inside a static magnetic island. A clear observation of low heat diffusivity inside the magnetic island is presented in this Letter.

The experiments are carried out in the LHD with a major radius at the magnetic axis of $R_{ax} = 3.5$ m, an averaged minor radius of $a = 0.6$ m, and a magnetic field at axis of up to 2.88 T [12]. Typical parameters in this experiment are the following: line averaged density $(1–2) \times 10^{19}$ m^{-3}, central electron temperature up to 1.5 keV, and heating power up to 2 MW with neutral beam injection. A 32-channel heterodyne radiometer is used to track the small electron temperature perturbations [13]. The second harmonic of the X mode is optically thick in typical LHD plasmas, and the electron temperature measured by electron cyclotron emission (ECE) agrees well with that by Thomson scattering in this experiment.

In order to produce a cold pulse inside or outside the magnetic island, a tracer encapsulated solid pellet (TESPEL) is injected into the LHD edge (TESPEL consists of polystyrene as an outer shell and tracer particles as an inner core [14]). The TESPEL ablates within 1 ms and provides a small amount of tracer impurity and cold electrons. They reduce the edge electron temperature ($\delta T_e/T_e < 10\%$) and then temperature perturbation usually propagates towards the core region (cold pulse propagation). The changes of the total stored energy and the electron density in the core region are negligible. The particle diffusivity (≤ 0.1 m^2/s), which is estimated by gas-puff modulation experiment [15], is much smaller than the typical electron heat diffusivity (~ 1 m^2/s) in the LHD. Thus the electron heat transport dominates the particle transport in cold pulse propagation.

The size and phase of the static magnetic island ($n/m = 1/1$) can be controlled by changing the currents of the external perturbation coils, I_{pert}; here n and m are the toroidal and the poroidal mode number, respectively. Figure 1(a) shows the radial profile of the electron

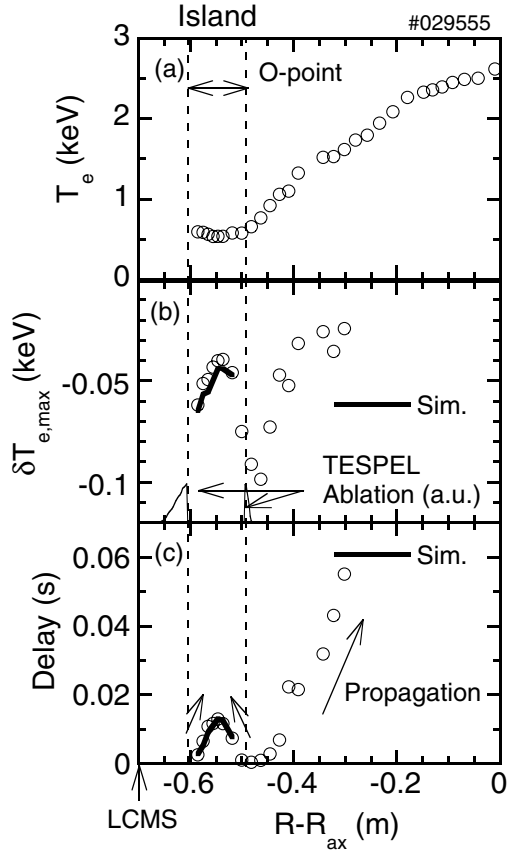

FIG. 1. Electron temperature perturbation induced by the TESPEL injection across the X point of the island. The radial profiles of (a) electron temperature before TESPEL injection, (b) peak of the cold pulse and the intensity of the ablation light of TESPEL, and (c) delay of time to peak of the cold pulse. Here R is the major radius and the last closed magnetic surface is at $R - R_{\rm ax} = -0.7$ m. Note the ECE receiving antenna is mounted at the inboard side of the LHD.

temperature with an island ($I_{\rm pert} = 800$ A) just before the TESPEL injection. The flattening of the electron temperature profile appears in the edge region where the O point of the magnetic island is located. In this experiment, the beam deposition power inside the island is less than 6% of the total power deposited to plasma, which is not enough to produce a peaked electron temperature profile inside the island. The TESPEL is injected from the outboard side only 72° toroidally from the ECE antenna. Therefore, the TESPEL can be injected across the X point of the island. Figure 1(b) shows the radial profile of the peak of the cold pulse; here the peak of the cold pulse is defined as the maximum magnitude of the electron temperature perturbation at each radius, $\delta T_{e,\rm max}$ (usually negative). The projection of the intensity of the TESPEL ablation light (H_α) into the radial position is also indicated in Fig. 1(b). Because the TESPEL ablates just outside the island, the peak of the cold pulse is the largest near the boundary of the island. Figure 1(c) shows the delay of time to peak of the cold pulse with respect to the time to peak of the cold pulse of the boundary of the island ($R - R_{\rm ax} = -0.48$ m), where the electron temperature drops most rapidly after TESPEL injection. The delay of the time to peak reveals that the cold pulse propagates inward (to the core region) and outward (to the O point of the island). The delay of the cold pulse at the same magnetic surface inside the island is identical as shown in Fig. 1(c). The peak of cold pulse decreases monotonically as it propagates toward the O point. This suggests that the heat transport is diffusive (not involved with inward pinch [16]). The simulation results shown in Figs. 1(b) and 1(c) are discussed later.

To study the cold pulse propagation near the X point, the phase of the island is reversed by changing the polarity of $I_{\rm pert}$ ($I_{\rm pert} = -1200$ A). In this case, the ECE system views the X point of the island. Because the boundary of the island is indistinct due to the increase in the stochastic region near the X point of the island, the flattening of the temperature profile is unclear from the ECE measurement (other diagnostics, e.g., the ion temperature profile show

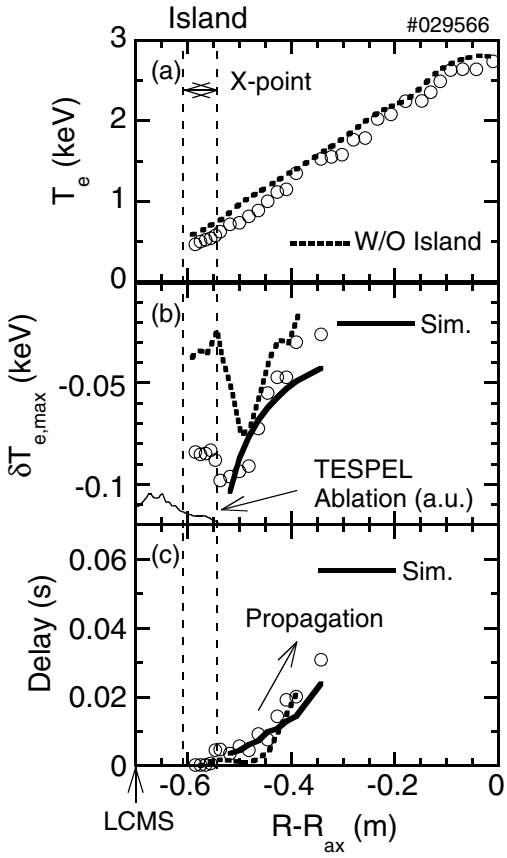

FIG. 2. Electron temperature perturbation induced by the TESPEL injection into the O point of the island. The radial profiles of (a) electron temperature before TESPEL injection, (b) peak of the cold pulse and the intensity of the ablation light of TESPEL, and (c) delay of time to peak of the cold pulse. A result obtained without island is also shown as a broken line.

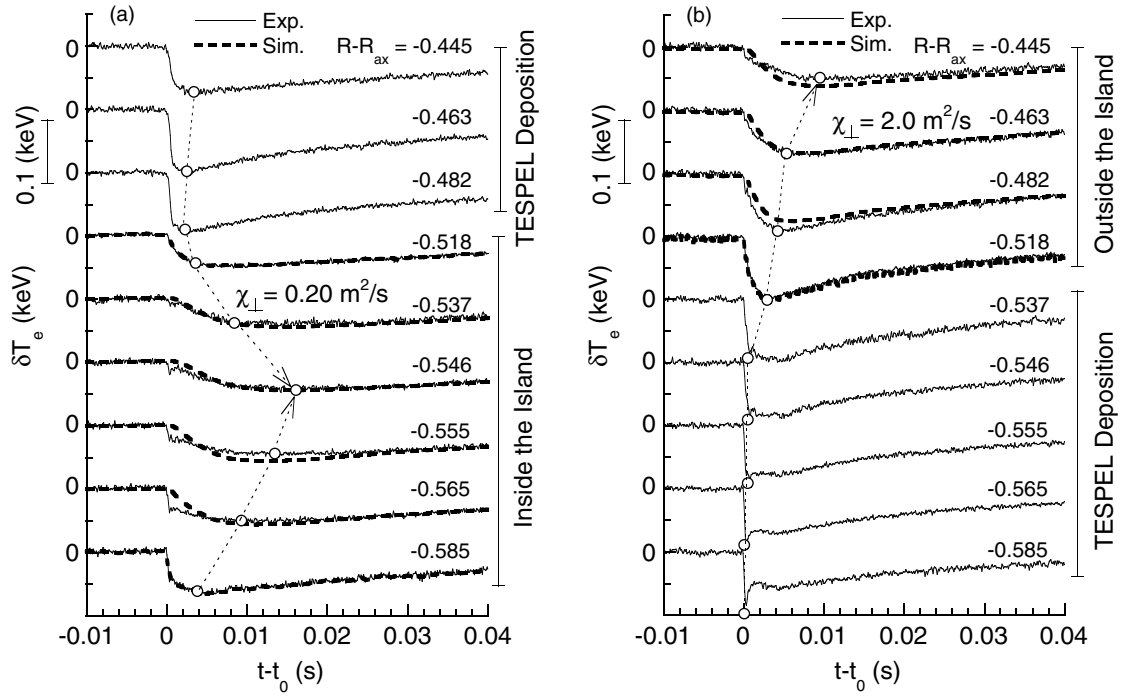

FIG. 3. Comparison of temperature perturbation between experiment and simulation. The time evolutions of the measured (sold line) and the simulated (broken line) temperature perturbation at different radii in the same discharges as (a) Fig. 1 and (b) Fig. 2, respectively.

the flattening at the O point of the island). The TESPEL is injected into the O point of the island and ablated inside it and then the cold pulse is induced just outside the island as shown in Fig. 2. The pulse propagation outside the island is compared with that inside the island to clarify the difference in heat transport. Because the electron temperatures of the target plasmas are almost the same in the region where the cold pulse propagates (0.6 keV inside the island in Fig. 1 and 0.7 keV within the region of -0.5 m $< R - R_{\rm ax} < -0.45$ m in Fig. 2), the dependence of the heat diffusivity on the temperature can be neglected with regard to the comparison of the heat transport in this experiment. The temperature profile and cold pulse propagation without any islands are also shown in Fig. 2. The stored energy with island is smaller than that without island by 20% which is identical to the fraction of area inside the magnetic island to the total cross section. The temperature gradients in the vicinity of the X point are almost the same as that without an island. This indicates the local confinement is unchanged by the presence of an island in this experiment. Certainly, the cold pulse outside the island propagates similarly to that without any islands.

Figure 3 shows the time evolutions of the electron temperature perturbation at different radii in both cases of Figs. 1 and 2. The TESPEL is injected at time $t = t_0$. The simulation results with a simple diffusion model are also shown. In this simulation, the perturbation equation written as

$$\frac{3}{2} n_e \frac{\partial \delta T_e}{\partial t} = \nabla \cdot (n_e \chi_\perp \nabla \delta T_e), \tag{1}$$

is solved numerically by using the time dependent boundary condition. Here δT_e is the temperature perturbation, n_e is the electron density, and $\chi_\perp$ is the heat diffusivity across the magnetic field, respectively. Homogeneous $\chi_\perp$ and electron density are assumed and the electron density perturbation is neglected. The slab and the cylindrical geometry are used for simplicity. The best fit of the simulation to the observation gives $\chi_\perp = 0.2$ m^2/s inside the island [Fig. 3(a)] and $\chi_\perp = 2.0$ m^2/s outside the island [Fig. 3(b)], respectively. These simulation results clearly indicate that the heat diffusivity inside the island is much smaller than the one outside the island. The three-dimensional structure of the magnetic island should be included in the analysis to estimate the absolute value of the heat diffusivity more precisely.

The reduction of the heat diffusivity inside the island is also observed in an island of a different size. Figure 4 shows the cold pulse propagation inside the island for plasmas with various sizes of the island. Here τ is the delay of the time to peak of the cold pulse, $\Delta R = |R - R_{\rm b}|$ is the propagation length of the cold pulse, $R_{\rm b}$ is the location of the boundary of the island, and $W_{\rm I}$ is the island width, respectively. The pulse propagation outside the island is also shown in Fig. 4. The heat diffusivity can be estimated as $\chi_\perp \sim c(\Delta R)^2/\tau$ by using the time-to-peak method [17]. Here the constant c depends on the

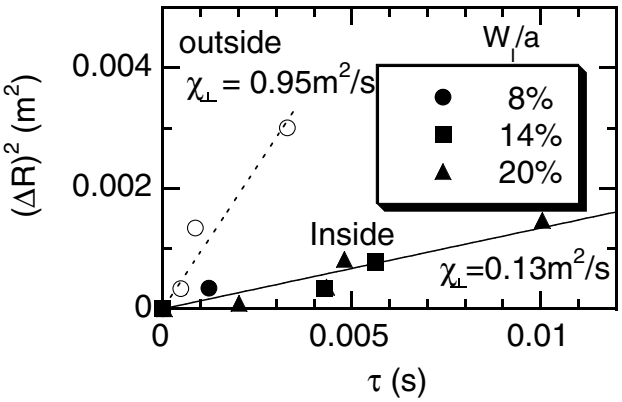

FIG. 4. Cold pulse propagation for plasmas with various sizes of the island. The closed symbols indicate the propagation inside the island and the open circles indicate the propagation outside the island.

boundary condition and is set to unity for simplicity (the boundary condition is given by a delta function). Thus the slopes of the plots in Fig. 4 give the heat diffusivity. The thermal diffusivity estimated inside the island is 0.13 m^2/s and is smaller than that estimated outside the island (~ 0.95 m^2/s), which is consistent with the simulation results shown in Fig. 3. The fact that data points for different sizes of magnetic island are on one line indicates that the heat diffusivity inside the island does not depend on the size of the island. It is indicated that a finite ratio of $\chi_\perp/\chi_\parallel$ leads to a critical island size W_c, above which T_e flattening inside the island appears [8]. Here $\chi_\parallel$ is the parallel heat diffusivity. The value of critical size W_c is estimated to be 0.2 cm using $\chi_\perp = 0.2$ m^2/s. The actual island size $W_I/2$ is 2 cm when $W_I/a = 8\%$ and thus is much larger than W_c. The island size is also much larger than the orbit width for helically trapped electrons (0.03 cm) and protons (0.4 cm).

A heavy ion beam probe measurement in Texas Experimental Tokamak shows a reduction of the density fluctuation level in the O point of the island [18]. Thus, the reduction of heat diffusivity inside the island is considered to be due to the small level of the turbulence driven transport. The flattening of the pressure profile itself suggests no pressure gradient driven mode. This means that the profile flattening and the reduced heat diffusivity inside the island are self-conservative. The possibility of multiequilibrium and their bifurcations inside the island are predicted by theories [19,20]. The profile flattening involving reduced heat diffusivity may be one of the stable states inside the island as well as the density peaking in "snake" modulation [4] and the formation of radial electric field structure [3]. Even in a rotating island, the heat diffusivity can be as small as that inside the static island. In conclusion, the heat transport inside the island in the LHD is investigated by using cold pulse propagation induced by TESPEL injection. The experimental results show (i) the heat diffusivity inside the island is reduced by 1 order of magnitude and (ii) the heat diffusivity inside the island does not depend on the size of the island.

We are grateful to the technical group for their excellent support. We thank Professor K. Itoh for helpful discussions.

[1] J. A. Snipes *et al.*, Nucl. Fusion **30**, 205 (1990).
[2] H. Zohm *et al.*, Nucl. Fusion **41**, 197 (2001).
[3] K. Ida *et al.*, Phys. Rev. Lett. **88**, 015002 (2002).
[4] A. Weller *et al.*, Phys. Rev. Lett. **59**, 2303 (1987).
[5] Y. Nagayama *et al.*, Phys. Plasmas **3**, 2631 (1996).
[6] K. Narihara *et al.*, Phys. Rev. Lett. **87**, 135002 (2001).
[7] B. P. V. Milligen *et al.*, Nucl. Fusion **33**, 1119 (1993).
[8] R. Fitzpatrick, Phys. Plasmas **2**, 825 (1995).
[9] M. R. de Baar *et al.*, Phys. Rev. Lett. **78**, 4573 (1997).
[10] P. Mantica *et al.*, Phys. Rev. Lett. **82**, 5048 (1999).
[11] N. Ohyabu *et al.*, Phys. Rev. Lett. **88**, 055005 (2002).
[12] M. Fujiwara *et al.*, Nucl. Fusion **41**, 1355 (2001).
[13] Y. Nagayama *et al.*, Rev. Sci. Instrum. **70**, 1021 (1999).
[14] S. Sudo *et al.*, Plasma Phys. Controlled Fusion **44**, 129 (2002).
[15] K. Tanaka *et al.*, J. Plasma Fusion Res. **4**, 427 (2001).
[16] H. W. Drawin *et al.*, Nucl. Fusion **32**, 1615 (1992).
[17] M. W. Kissick *et al.*, Nucl. Fusion **34**, 349 (1994).
[18] P. M. Schoch *et al.*, in *Proceedings of the 15th European Conference on Controlled Fusion and Plasma Heating* (European Physical Society, Dubrovnik, 1988), Vol. 12B, Pt. I, p. 191.
[19] S. I. Itoh and K. Itoh, Comments Plasma Phys. Controlled Fusion **13**, 141 (1990).
[20] K. C. Shaing, Phys. Plasmas **9**, 3470 (2002).